Advances in Science and Technology Research Journal

Advances in Science and Technology Research Journal, 2026, 20(7), 505–520
https://doi.org/10.12913/22998624/219961
ISSN 2299-8624, License CC-BY 4.0

Received: 2026.02.13
Accepted: 2026.05.15
Published: 2026.06.01

Experimental evaluation of seat belt mechanics under dynamic impact

Maciej Obst[1*], Szymon Rzepczyk[2], Dariusz Kurpisz[1], Sebastian Głowiński[3]

[1] Institute of Applied Mechanics, Poznan University of Technology, ul. Jana Pawła II 24, 60-965 Poznan, Poland
[2] Department of Forensic Medicine, Poznan University of Medical Sciences, ul. Rokietnicka 10, 60-806 Poznan, Poland
[3] Institute of Health Sciences, Slupsk Pomeranian University, Westerplatte 64, 76-200 Slupsk, Poland
* Corresponding author's e-mail: maciej.obst@put.poznan.pl

ABSTRACT

Although the basic principle of seatbelts operation has changed little since their introduction as mandatory equipment, the continuous integration of seat belts with other safety systems has created new challenges in their design, testing, and evaluation. This study provides an experimental investigation into the dynamic mechanical behaviour of seat belt webbing, with particular emphasis on its energy dissipation capacity under impact conditions. Novel aspects of this work include a comparative evaluation of new belts and intentionally degraded belts, enabling a phenomenological assessment of how defects influence load response and potential injury risk. Energy characteristics were employed as comparative indicators, providing an interesting complementary diagnostic measure. Dynamic impact tests were performed using a high-speed camera system to capture displacement-time histories, and mathematical functions approximating the experimental data were proposed with strong agreement to measurements. The results highlight underexplored differences in webbing performance under defective conditions, providing new insights relevant to regulatory compliance and the development of advanced restraint systems.

Keyword: seat belts, injury prevention, crashworthiness, impact energy.

INTRODUCTION

The primary means of passive protection for vehicle occupants is the well-known three-point seat belt (Developed by Nils Bohlin and introduced in Volvo vehicles in 1959). Its widespread use significantly reduces the consequences of road accidents, and in most countries, the wearing of seat belts is a legal requirement for all passengers. The origins of seat belt technology can be traced back to the mid-nineteenth century, although the modern three-point design was first implemented in cars in the mid-twentieth century.

Recent decades have brought considerable technological progress in seat belt systems, with a growing role of mechatronic solutions [1]. Modern systems, equipped with sensors and actuators, are capable of adapting their performance to the circumstances of an accident. Nevertheless, even highly advanced restraint systems cannot guarantee complete protection, as seat belts themselves may contribute to certain injuries—particularly when they are improperly used [2]. The key structural element ensuring the protective function of the seat belt is the webbing, typically woven from nylon or polyester fibers. Analyzing its mechanical properties and deformation under static and dynamic loading provides valuable insights into both occupant biomechanics and potential injury mechanisms. In this context, experimental and analytical studies of seat belt webbing enable the development of dynamic mechanical characteristics that are directly relevant to crash safety. Although the medical literature [3] includes reports of injuries associated with seat belt use, such injuries are generally far less severe than those sustained by unbelted occupants. Continued improvements in seat belt design must therefore be carried out in close collaboration with clinical medicine, particularly in disciplines with direct contact with road traffic accident victims.

Constructions of seat belts systems

A seat belt system consists of the following elements: retractor, buckle, webbing, pyrotechnic pretensioner, and guiding loops. The main component of the system is the webbing, usually made of polyester or nylon fibers, whose function is to dissipate the kinetic energy of the protected passenger's body in a way that maximizes the chances of survival while minimizing injuries. Nowadays, high-strength fabrics reinforced with carbon or aramid fibers can also be found, offering improved protective performance for passengers [4]. Interestingly, the regulations governing the requirements for automotive seat belts do not explicitly define the material to be used for the webbing [5]. The most widely used seat belt in passenger cars is the three-point belt system. The anchorage points of the three-point belt are located near the passenger's hips and shoulder. This solution is relatively convenient in everyday use. The retractor, or winding mechanism, is located at one end of the belt and is responsible for maintaining appropriate belt tension during use, ensuring proper fit to the passenger's body. The buckle and latch (tongue plate) allow fastening of the belt, serving also as an anchorage point. The buckle consists of a locking mechanism that engages with the latch. Modern seat belts are commonly equipped with a pyrotechnic pretensioner, a device that instantaneously tightens the belt in the event of a crash. The pretensioner stabilizes the protected passenger in the seat, reducing forward displacement and limiting impact against the belt and vehicle interior. The guiding loop, mounted on the vehicle's B-pillar or integrated into the seat backrest, ensures proper positioning of the belt. Seat belt webbings are manufactured with different fibber weaves. The most common types include unidirectional and bidirectional weaves [6–8]. Unidirectional weave provides high tensile strength along the length of the belt and favourable mechanical characteristics, while bidirectional weave ensures both longitudinal and transverse strength. Apart from the three-point belt, other types exist, including two-, four-, five-, and six-point belts. The two-point belt provides insufficient protection for the head and chest [9]. The three-point belt represents a compromise between user comfort and effective restraint. The four-point belt ensures improved stabilization of the body and is used mainly in sports and racing cars. The five-point belt is widely used in sports cars, off-road vehicles, and child safety seats. The six-point belt represents the most advanced restraint system, utilizing two lap straps and two shoulder straps that pass through additional anchorage points on the seat or seat frame.

Prevention and injury

Seat belts represent one of the key protective elements in vehicles, particularly during road traffic accidents [10]. Studies have shown that individuals who do not wear seat belts have more than five times higher risk of sustaining severe injuries and more than eight times higher risk of death compared with those wearing seat belts [11]. Several factors influence the protective effectiveness of seat belts: type of construction and number of anchorage points, presence of auxiliary equipment (e.g., pretensioners), correct installation and adjustment to the passenger's body size, and type of collision [12,13]. Properly functioning three-point seat belts distribute the body's kinetic energy during a collision to areas less prone to injury, transferring forces to the anchorage points. By restraining the upper torso, they prevent excessive forward displacement, subsequent hyperflexion of the spine, and head impact against interior elements [12,14]. They also reduce the risk of passenger ejection from the vehicle [14]. This is particularly critical for front-seat occupants, where head impact against the steering wheel, dashboard, or windshield—rigid elements—can result in severe or fatal cranio-cerebral trauma [12,14]. Incorrectly adjusted or improperly fastened seat belts may lead to significant reduction in protective effectiveness due to the risk of "submarining" (sliding under the belt) during a crash. Despite the unquestionable benefits of seat belts, the forces generated during crashes may themselves contribute to injuries, even when the belt is correctly fastened [15,16]. The spectrum of injuries resulting from seat belt use during traffic accidents is referred to as seat belt syndrome (SBS) [14,17]. This includes both external and internal injuries [12]. External injuries typically present as bruises and abrasions aligned with the path of the belt, known as the seat *belt sign* [12]. This phenomenon is more pronounced in obese individuals, due to crushing of vascularized subcutaneous fat tissue. Clinically, the seat belt sign is significant, as its presence correlates with increased risk of internal organ injury, and it is also useful in crash reconstruction to determine occupant position [12,18–20].

Study of seat belt systems and test methods

The methodology for testing seat belt systems, as defined by current legal regulations, is specified in UN Regulation No. 16. In the European Union, Directive 2007/46/EC describes homologation conditions for motor vehicles. Industry testing can generally be divided into full system testing and component-level testing. Full system testing is conducted using dedicated test benches or by evaluating entire vehicles, such as in crash tests. The loading mechanisms acting on the restrained human body are studied using anthropomorphic test devices (dummies), human cadavers, volunteers, and computer simulations. In dynamic cadaver testing, a novel stress measurement technique has been developed using uniaxial and rosette strain gauges placed on the rib cage [21]. This methodology

enabled precise determination of the timing of individual rib fractures, which were shown to occur within the first 35% of chest compression and to be side-dependent. Experimental studies [22], demonstrated that airbags and seat belts play a key role in reducing forces acting on the body during frontal collisions. Simulating low-speed frontal crashes, researchers compared two-point versus three-point belts, showing that three-point belts reduced occupant displacement, shortened belt tensioning time by up to 0.1 s, and decreased head acceleration. Three-point belts also significantly reduced the risk of "submarining," which in two-point belts can reach ~10 cm [23]. Other studies [24], focused on tape retractor displacement and damage during prototype seat testing, highlighting anchorage force distribution and suggesting the use of previously worn belts for prototype evaluations. Crash testing of racing cars [25] against rigid barriers measured belt forces acting on dummies, applying the Gibbs-Appell method for analytical modeling of vibrational dynamics. Authors proposed integrating an energy absorber into belts, reducing peak belt forces. Investigations on Takata ABS plastic buckle release buttons (models 52 and A7) used in cars (1986–1991) revealed fatigue-related cracking and fragmentation due to design flaws, aggravated by the lack of reinforcing ribs [26]. Dynamic studies [27] compared two webbing types: standard TS and modified TM (both polyester-based, but differing in weave and geometry). Results showed that TM stretched more than TS under 200 mm extension at 0.1 m/min loading rate. Further research [28] examined dynamic strength of webbings (25.4 × 1.56 mm and 38.6 × 1.23 mm) in restraining a 15 kg child dummy at 50–52 km/h deceleration tests (28 g). Results indicated that belt stiffness at low loads was nearly twice as low as at 50% of ultimate strength, underlining its influence on the protective function of child restraints. The study [29] presents the results of numerical analyses simulating a passenger car crash, in which a person protected by a seat belt and an airbag is assessed using biomechanical injury criteria.

Despite the extensive knowledge on seat belt systems, relatively little attention has been devoted to the influence of thermal and mechanical degradation of seat belt webbing on its dynamic behaviour. Real-world usage exposes belts to elevated temperatures inside vehicles and to accidental mechanical damage such as cuts, both of which may compromise their protective effectiveness.

The main objective of this study is therefore to experimentally investigate the effect of thermal exposure and mechanical notching on the dynamic mechanical response of seat belt webbing under impact loading. The research aims to:

- Compare the deformation, strain rate, acceleration, and energy absorption characteristics of new, thermally degraded, and notched seat belt specimens.
- Evaluate how different levels of impact energy influence the response of each belt condition.
- Identify degradation-induced changes in the protective potential of seat belt webbings.

By addressing these objectives, the study seeks to provide deeper insight into the degradation mechanisms of seat belt webbings and their safety implications, offering useful guidance for both automotive safety regulations and the development of more durable restraint systems.

MATERIALS AND METHODS

Seat belt webbing specimens used in the experimental dynamic load tests are shown in Figure 1. The effective gauge length of each specimen (the distance between the grips) was 300 mm. For each loading case of the conveyor belt, a new specimen of the belt was used. Furthermore, for a single loading scheme, the experimental investigations were conducted on five belt specimens. The obtained experimental results (characteristics – displacements of individual markers as a function of time) were superimposed, which enabled their averaging and, consequently, the determination of the variable increments in length of the individual sections of the tested belt specimen. Dynamic impact tests were conducted using a drop tower equipped with dedicated grips and a reversing mechanism with sliders, enabling the application of tensile loading to the webbing upon impact. A schematic of the test stand is shown in Figure 2, where the inertia mass of the impactor directly interacts with the seat belt specimen. The impact load was generated using a 5 kg impactor, while displacements of the gauge section were recorded with a high-speed Chronos 2.1-HD camera operating at 7135 fps.

RESULTS

Figure 3A–C shows the dynamic elongation curves of the seat belt specimens, expressed as Δl [mm] as a function of time t [s], obtained during impact tests with different drop heights of the impactor: 1 m, 1.5 m, and 2 m. These heights correspond to different strain rates in the webbing and different levels of impact energy. Three

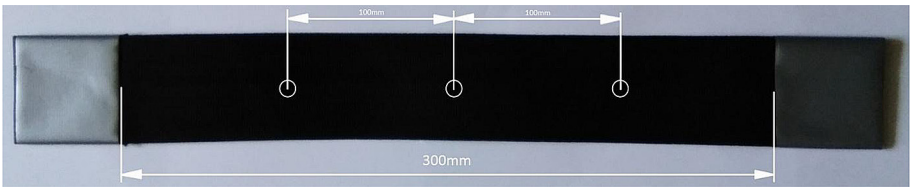

Figure 1. Car seat belt webbing specimen

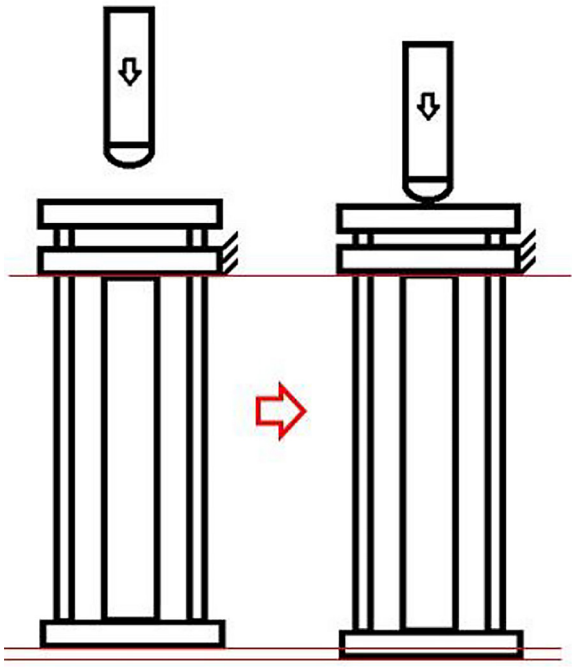

Figure 2. Schematic of the drop tower setup used for dynamic loading of the seat belt webbing specimen

measurement markers were applied along the specimen, allowing the experimental determination of elongation increments in three specific gauge sections: 0–100 mm, 100–200 mm, and the averaged response over the entire 0–200 mm length (denoted as 0–200/2). This approach made it possible to assess the influence of the distance between the dynamic loading point (connection of the moving part of the reverser with the specimen) and each section of the tested belt on the resulting deformation characteristics. The experimental displacement curves were approximated using a three-parameter family of functions of the form:

$$\Delta l(t) = b \cdot sin^n(ct) \quad (1)$$

where: parameters b, c and n were individually fitted to each experimental curve. This formulation facilitated straightforward derivation of velocity and acceleration according to:

$$V(t) = bcn \cdot sin^{n-1}(ct) \cdot \cos(ct) \quad (2)$$

$$a(t) = \frac{dV}{dt} = bc^2n(n-1)sin^{n-2}(ct) - c^2n^2\Delta l(t). \quad (3)$$

Figure 3A presents the results for the 1 m drop height. Elongation systematically increased over time, reaching approximately 6 mm at its maximum. The elongation was not uniform across the three measurement sections, confirming the influence of gauge location. Nevertheless, the fitted approximation functions ("0–100A" and "100–200A") showed good agreement with the experimental data. Figure 3B shows the results for the 1.5 m drop height. In this case, the elongation increased significantly, reaching values of about 11 mm, indicating more intense stretching of the webbing due to higher impact energy. The differences between the 0–100 mm and 100–200 mm sections also became more pronounced. As before, the approximation functions closely matched the experimental results. Figure 3C presents the results for the 2 m drop height. Interestingly, despite the higher impact energy, the maximum elongation decreased slightly to around 7 mm. This suggests that the tested webbing exhibited sensitivity to strain rate. Once again, the close agreement between the experimental data and the fitted functions confirms the suitability of the chosen approximation family and the regular nature of the dynamic deformation process.

Figure 4 presents the elongation behaviour of seat belt webbing subjected to prior conditioning, specifically heating in a thermal chamber to approximately 60 °C in accordance with UN Regulation No. 16. The accompanying thermographic image (Figure 4) confirms a uniform temperature distribution in the belt prior to testing. After testing, the thermal image was recorded once the belt had cooled considerably. Dynamic tensile impact tests were then carried out for three drop heights of the impactor: A – 1 m, B – 1.5 m, and C – 2 m. Compared with the unheated (new) belt, the thermally conditioned belt exhibited greater elongation under lower impact energy (Figure 4A). For example, at a 1 m drop height, elongation reached

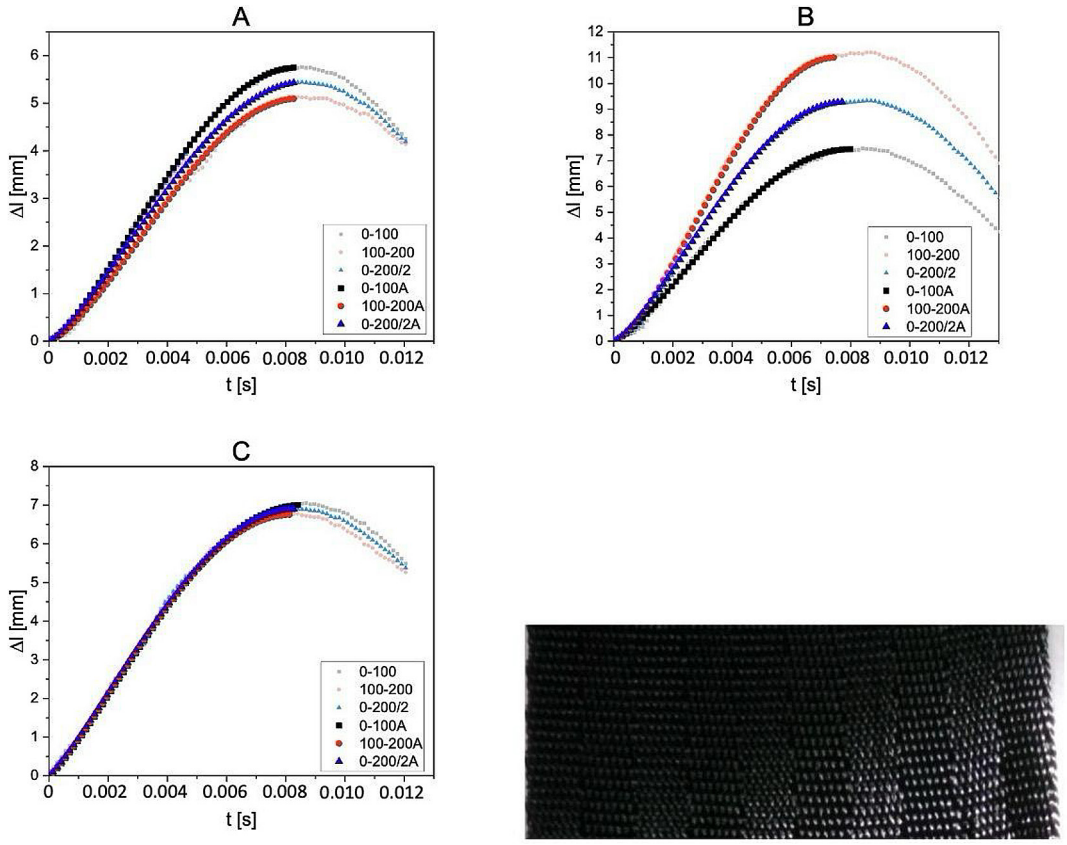

Figure 3. Dynamic elongation of a new seat belt under impact loads from different drop heights: A – 1 m; B – 1.5 m; C – 2 m

approximately 6.5 mm, whereas the unheated belt extended only about 6 mm. In addition, the elongation curves of the heated strip showed an uneven course in all test cases (A–C, Figure 4), suggesting partial plastic deformation of the material under thermal exposure. This interpretation is supported by the observation of reduced initial stiffness, as indicated by steeper initial slopes of the elongation-time curves compared to those of the unheated belt. At higher drop heights, such as 2 m (Figure 4C), the differences between heated and unheated tapes are still clear. This result suggests that at higher impact energies, deformation depends on the internal structure of the fibers and their thermal state. In all cases, the approximation functions (curves labelled "A") demonstrated good agreement with the experimental measurements, further validating the chosen modeling approach.

Figure 5 presents the results of dynamic elongation tests performed on seat belt webbing with a pre-existing defect in the form of a transverse cut, 10 mm deep, made perpendicular to the webbing edge. A photograph of the cut location before testing is included in the lower corner of the figure. The results clearly demonstrate the significant influence of the defect on the mechanical properties of the belt, particularly in the progression of the experimental elongation curves, which lose their regularity. This effect may be attributed to fibber rupture mechanisms occurring in the vicinity of the notch tip. Across all impact energies, the maximum elongation values were lower compared to both the new and thermally conditioned belts (e.g., at 1 m drop height: ~3.8 mm for the cut belt, versus ~5.8 mm for the new belt and ~6.5 mm for the heated belt). Elongation also progressed in a more linear fashion and reached its maximum more rapidly, indicating reduced elasticity and earlier onset of damage. At the highest impact energy (2 m drop height, Figure 5C), the curves were more similar to each other, suggesting that under strong loading conditions, the effect of the defect is partially masked by the dominant influence of kinetic energy. The applied approximation functions (curves labelled "A") reproduced the experimental data with acceptable accuracy, confirming the suitability of this method for analysing weakened textile structures.

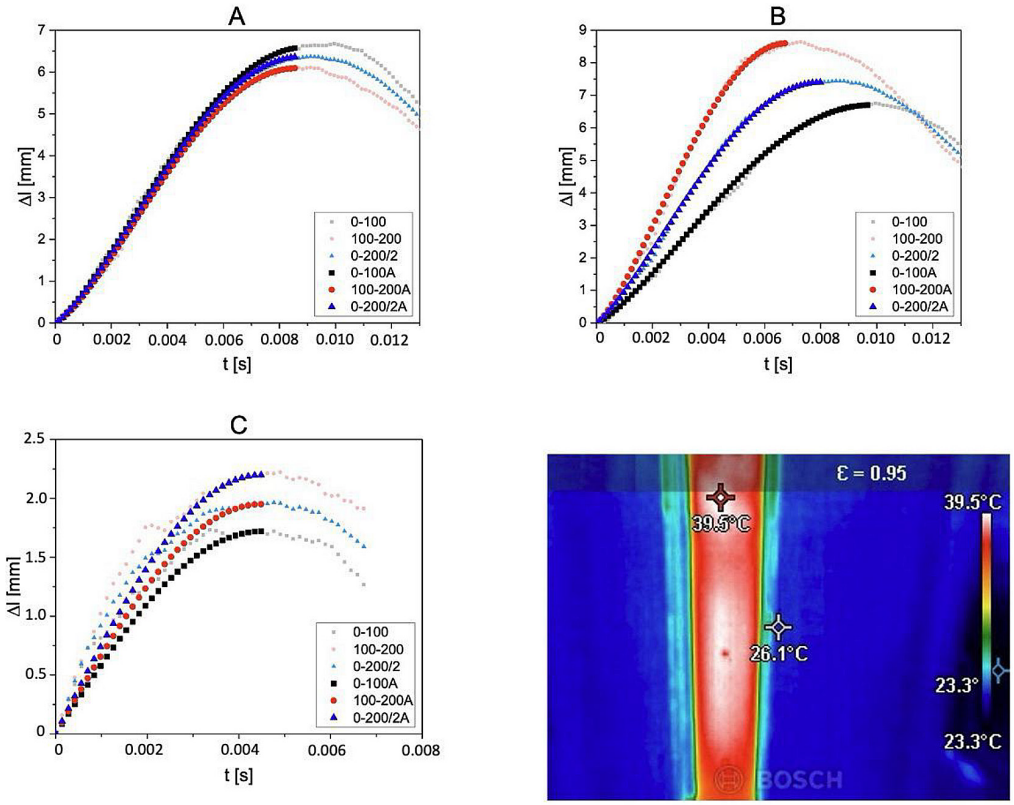

Figure 4. Dynamic elongation of thermally conditioned seat belt webbing under impact loads from different drop heights: A – 1 m (4.43 m/s); B – 1.5 m (5.42 m/s); C – 2 m (6.25 m/s). Thermographic image confirms homogeneous pre-test temperature distribution

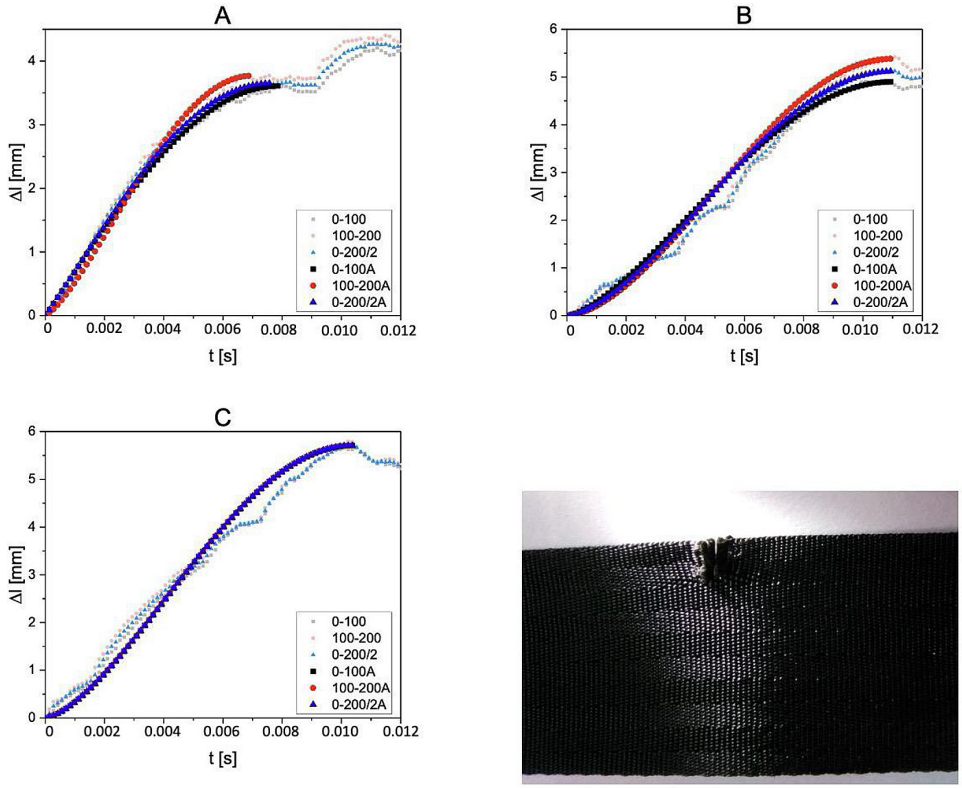

Figure 5. Dynamic elongation of cut seat belt webbing under impact loads from different drop heights: A – 1 m; B – 1.5 m; C – 2 m. Photograph shows the notch location prior to testing

Table 1 summarizes the key results obtained for the three types of seat belts tested. The belt exposed to elevated temperature exhibited the greatest susceptibility to deformation, most likely due to reduced stiffness caused by local plastic deformation of the fibers. Notably, however, an increase in stiffness was observed at the highest impact energy. The cut belt showed lower elongation than the new belt, indicating local structural weakening and a reduced capacity for energy absorption, which may represent the most hazardous condition from the perspective of user protection. The new belt was characterized by high elongation and no signs of degradation, confirming its full functionality. Figures 6A–C show the elongation velocity curves of the new belt as

Table 1. Comparison of maximum elongation of seat belts under different conditions and impact energies

Drop height	Condition	Maximum elongation Δl [mm]	Characteristics of deformation
1 m	New	~ 5.8	Smooth increase, distinct peak
	Heated	~ 6.5	Higher elongation, uneven deformation of the measuring section
	Cut	~ 3.8	Lower values, local irregularities; reduced cross-section leads to localized stiffening and fiber reinforcement
1.5 m	New	~ 11	Increased elongation, clear differences between markers
	Heated	~ 8.5	Lower values than new belt, clear differences between markers
	Cut	~ 5.4	Stable but lower curves, possible secondary micro-damage
2 m	New	~ 7	Reduced elongation at high energy—possible dynamic weakening effects
	Heated	~ 2.3	Lowest values, very steep and rapid deformation
	Cut	~ 5.7	Stable elongation, no differences between markers

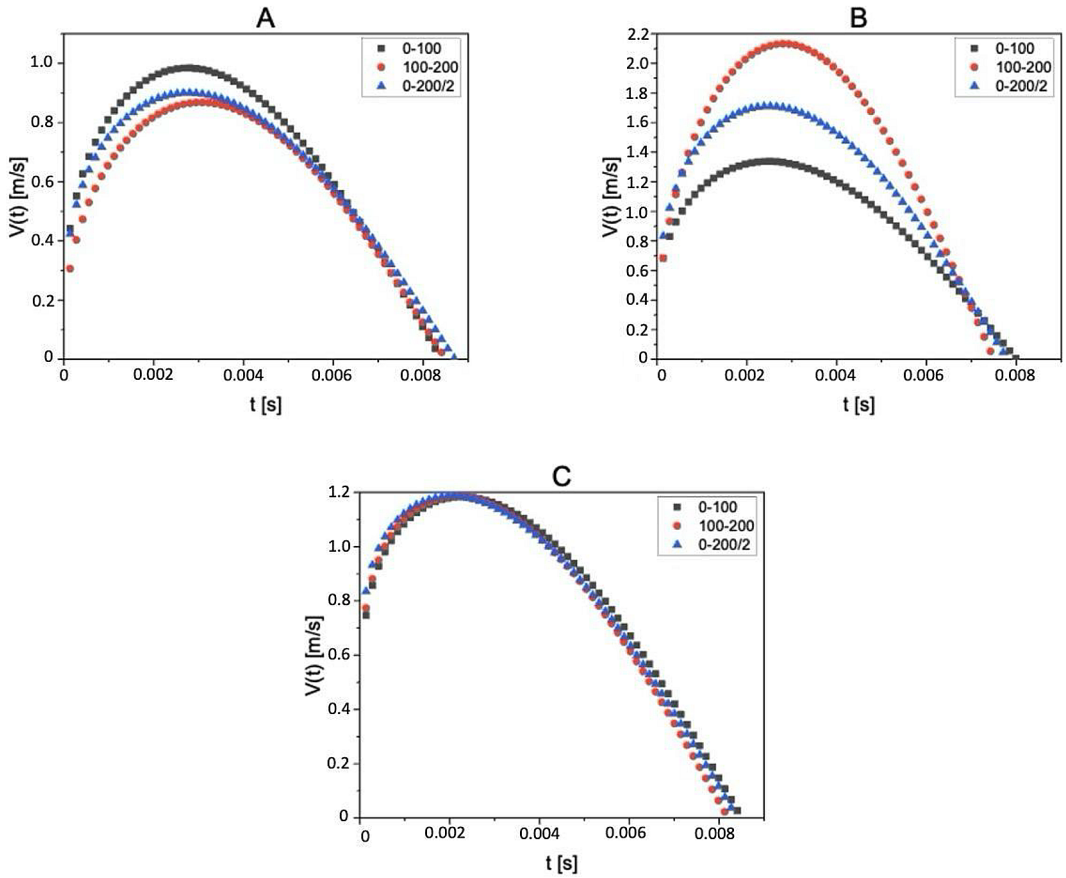

Figure 6. Velocity of elongation of the new seat belt under impact loads from drop heights of: A – 1 m; B – 1.5 m; C – 2 m

a function of time, obtained under impact loads from drop heights of 1 m (A), 1.5 m (B), and 2 m (C). For each series, three-gauge sections were analysed: 0–100 mm, 100–200 mm, and the averaged 0–200/2 mm. Increasing the drop height led to higher maximum strain velocities, most pronounced in Figure 6B. The results also revealed clear non-uniformities in strain velocity across the three-gauge sections. At the highest drop height (Figure 6C), however, the velocity curves nearly overlapped, suggesting that at higher energies, deformation becomes more uniformly distributed along the specimen length.

For the thermally conditioned belt (60 °C), clear differences in strain-rate characteristics were observed depending on the drop height of the impactor (Figure 7). At a 1 m drop height (Figure 7A), the curves displayed similar shapes and maximum values, suggesting a relatively uniform material response despite prior heating. The deformation progressed smoothly, with only minor differences between the measured gauge sections. At a 1.5 m drop height (Figure 7B), a distinct divergence appeared: the strain rate in the 100–200 mm section (red markers) reached significantly higher values and increased more rapidly. This behaviour may indicate localized material weakening in this region, potentially resulting from a loss of mechanical properties due to elevated temperature, or more specifically, increased sensitivity of the webbing to strain rate under these test conditions. At the highest drop height of 2 m (Figure 7C), the strain-rate curves were again more closely matched and nearly overlapping, suggesting that under high-energy impacts the material deforms in a more global and uniform manner, largely independent of prior heating. It is also possible that the belt reached a plastic state along its entire length, thereby masking earlier localized weaknesses. Overall, the variations observed may be attributed to thermal effects leading to partial softening of the webbing material and altering its elasto-plastic response to impulsive loading.

For the cut belt, the strain-rate curves (Figure 8) revealed an irregular and clearly disturbed profile, which is a typical consequence of localized structural damage. At the 1 m drop height (Figure 8A), a very rapid and abrupt deformation was

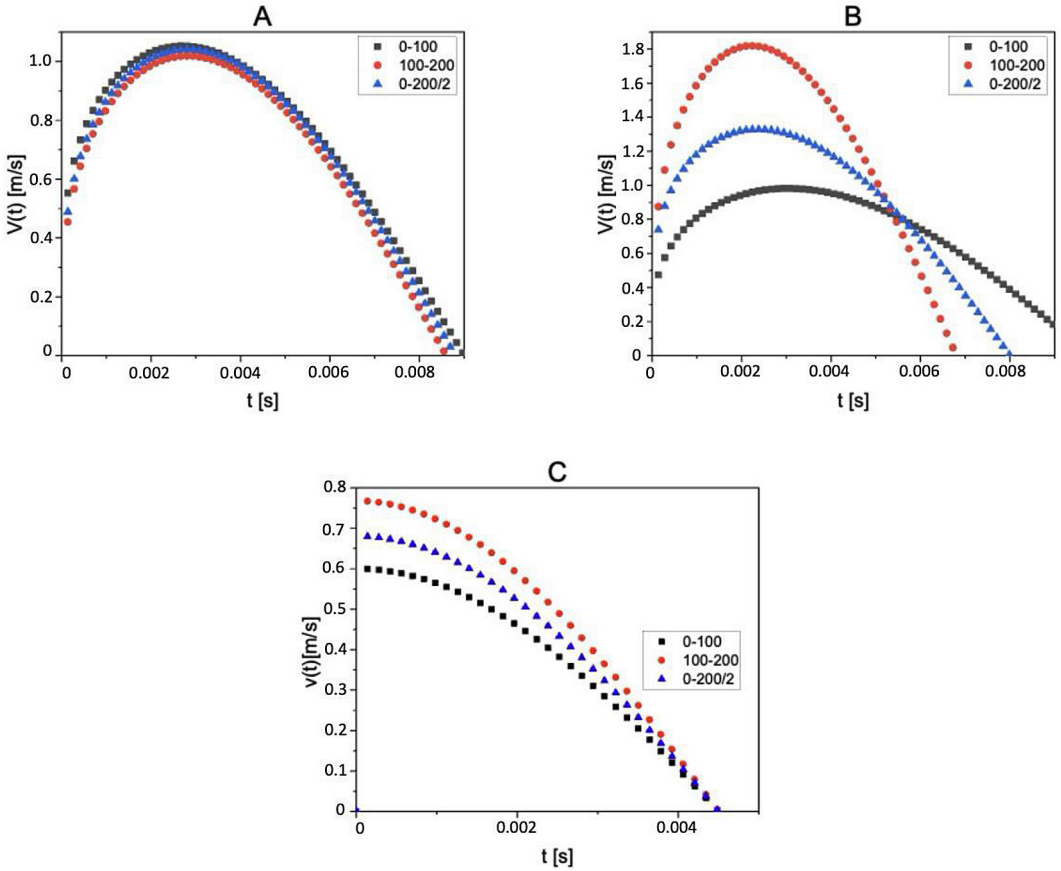

Figure 7. Strain rate of thermally conditioned seat belt webbing (60 °C) under impact loads from different drop heights: A – 1 m; B – 1.5 m; C – 2 m

observed in the 100–200 mm section (red markers), reaching higher maximum values than the other regions. This indicates that the notch was located in this section and significantly weakened the belt, leading to faster local deformation. In contrast, the curve for the 0–100 mm section (black squares) showed a delayed and lower response. At the 1.5 m drop height (Figure 8B), the curves became more similar, although the section containing the notch still exhibited the highest strain rate. This suggests that the weakening effect of the defect intensified with increased impact energy but was also partially redistributed across the remaining sections of the webbing. At the 2 m drop height (Figure 8C), the curves nearly overlapped, suggesting that at the highest energy level, the notch ceased to play a dominant role. In this case, the belt deformed more uniformly, possibly because the notch caused rapid localized failure, after which the remaining intact webbing absorbed the load and produced a more consistent strain-rate response. In summary, the presence of a notch strongly localized deformation under lower impact energies, substantially disturbing the belt's performance and potentially leading to premature failure or reduced occupant protection.

The acceleration responses of the seat belt specimens under dynamic loading are shown in Figures 9–11. For the new belt (Figure 9), the acceleration curves at all drop heights (A – 1 m, B – 1.5 m, C – 2 m) displayed a clear two-phase behaviour. In the initial phase, positive accelerations corresponded to momentum transfer from the impactor to the reverser. Subsequently, negative accelerations emerged, reaching their peak around 0.008 s, coinciding with the maximum elongation of the specimen. These negative values reflected the resistance of the webbing to further deformation. Increasing the drop height intensified both the magnitude of the accelerations and the rate of their development, indicating a stronger dynamic response of the belt material. For the heated belt (Figure 10), the acceleration characteristics were influenced by the prior conditioning at 60 °C. At the lowest drop height (1 m), the curves resembled those of the new belt but with slightly reduced negative acceleration values, suggesting diminished stiffness and increased

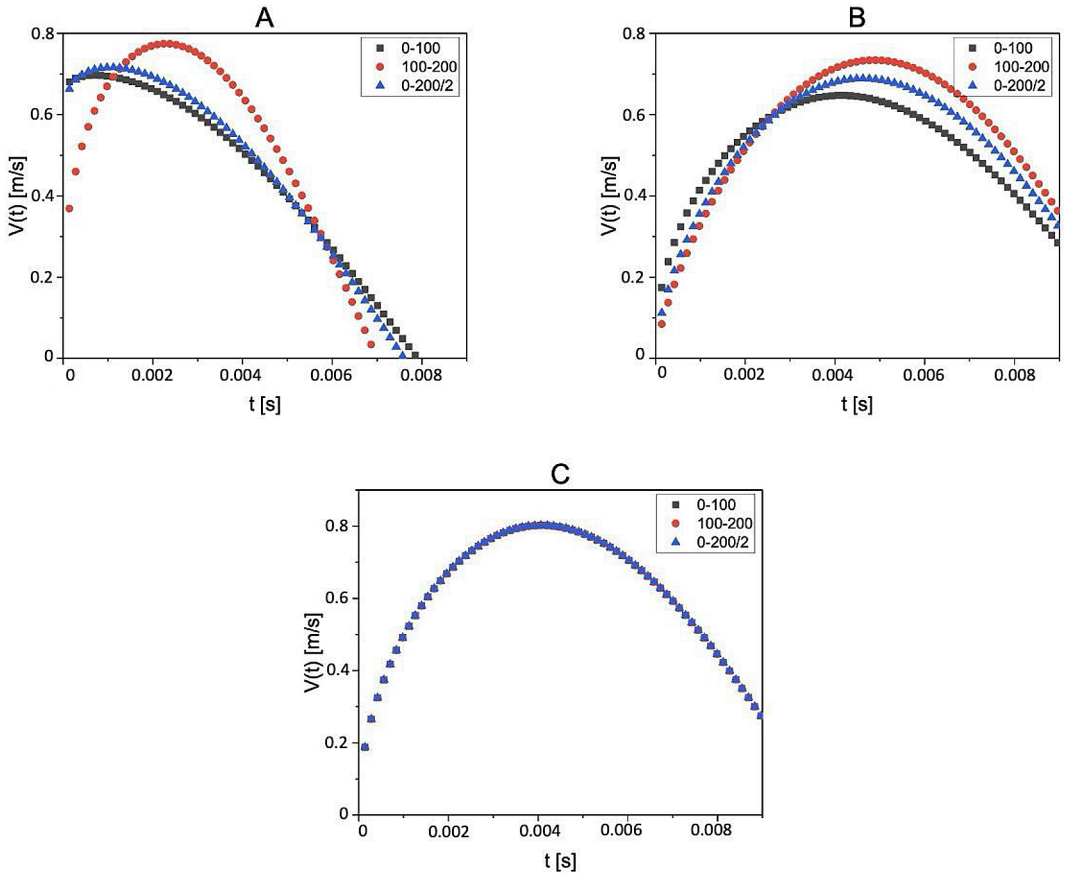

Figure 8. Strain rate of cut seat belt webbing under impact loads from different drop heights: A – 1 m; B – 1.5 m; C – 2 m

plasticity of the webbing. At 1.5 m and 2 m, the acceleration peaks became more irregular and less pronounced compared to the new belt, which may indicate localized material softening and a lower overall capacity to resist deformation under higher energy impacts. In the case of the cut belt (Figure 11), the acceleration responses exhibited the irregular patterns. At 1 m, negative acceleration values were markedly lower than those of the new and heated belts, consistent with the reduced elongation capacity and premature localization of deformation around the notch. At 1.5 m, the curves showed greater variability between tests, suggesting progressive fibber rupture in the vicinity of the defect. At 2 m, the acceleration profile approached that of the other belts, likely due to the dominance of global deformation mechanisms over local weakening. Nevertheless, the absolute values remained lower, confirming the impaired energy-absorbing capacity of the damaged belt.

Figure 12 presents the energy characteristics of the reverser–belt system for the new seat belt webbing, under the assumption of an elastic impact derived from the observed behaviour of the impactor and reverser. The energy was calculated using the following relation:

$$E(t) = \begin{cases} \frac{1}{2} \cdot m_R \cdot \left(V'^2_R - V^2_{R\_max}\right), \\ for\ t \le t_{max} \\ \frac{1}{2} \cdot m_R \cdot \left(V'^2_R - V^2_{R\_max}\right) - m_R \cdot a(t), \\ for\ t \ge t_{max} \end{cases} \quad (4)$$

where: V'_R and V_{R_max} denote, respectively, the theoretical reverser velocity determined from conservation of momentum and kinetic energy, and the actual velocity derived as the time derivative of displacement multiplied by 3, corresponds to the time at which the reverser reaches maximum velocity.

During the initial impact phase, when the reverser accelerates to its maximum velocity, energy transfer from the impactor to the reverser results in a steep increase in system energy. Once zero acceleration is reached, the system attains its maximum energy, which remains approximately constant, reflecting the gradual decrease in reverser velocity accompanied by increasing deformation work of the belt. At the highest drop height of 2 m (Figure 12C), the belt absorbed markedly higher energy—up to ~90 J. Notably, in the 0–200/2 mm section (blue triangles), the

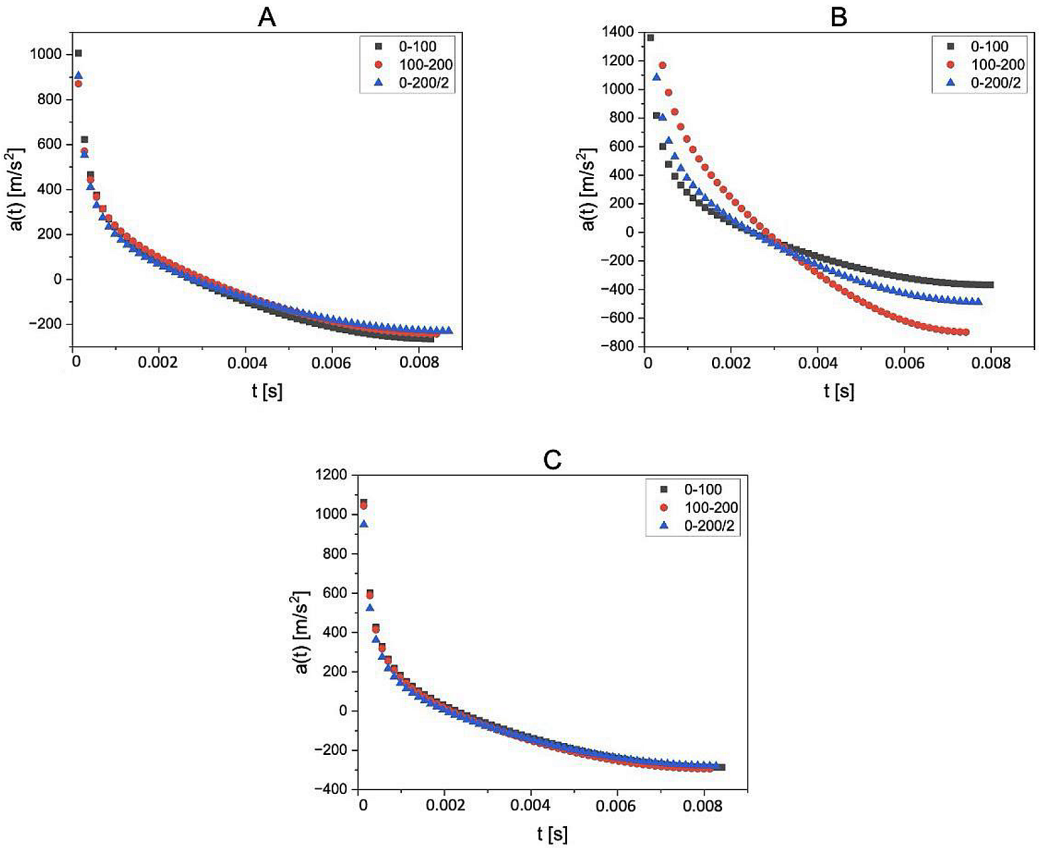

Figure 9. Acceleration of new seat belt webbing under impact loading at drop heights: A – 1 m; B – 1.5 m; C – 2 m

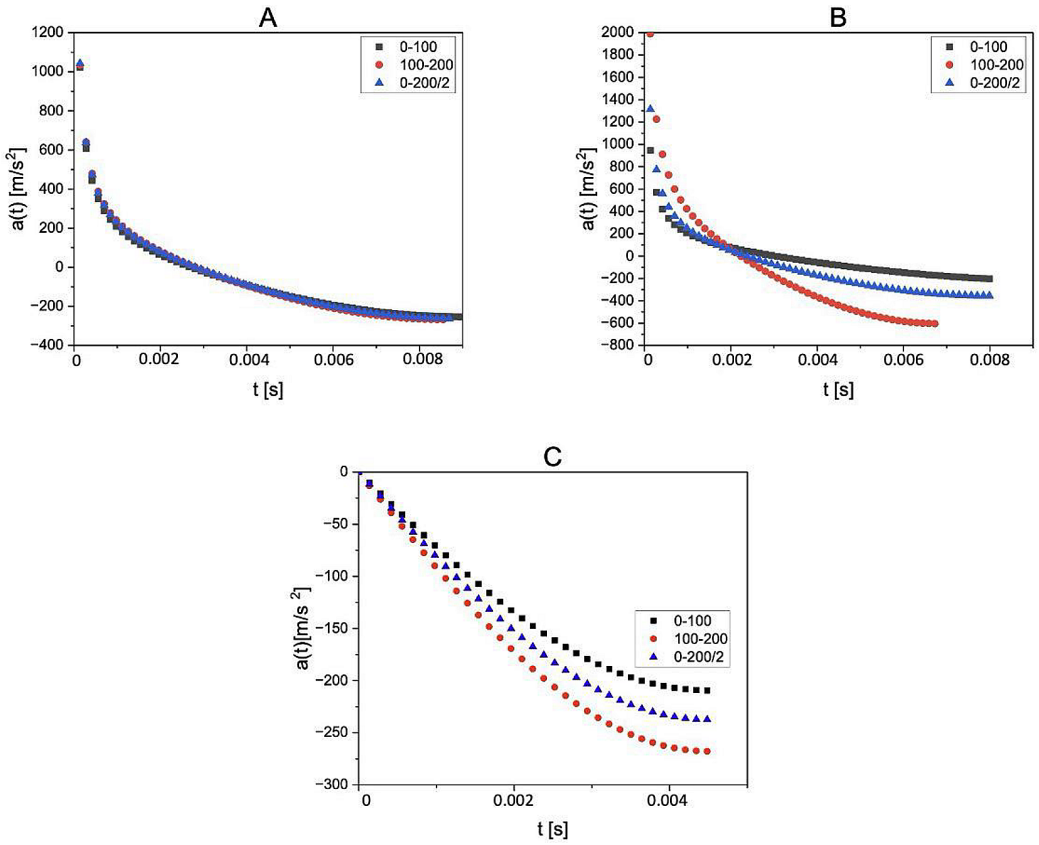

Figure 10. Acceleration of heated seat belt webbing under impact loading at drop heights: A – 1 m; B – 1.5 m; C – 2 m

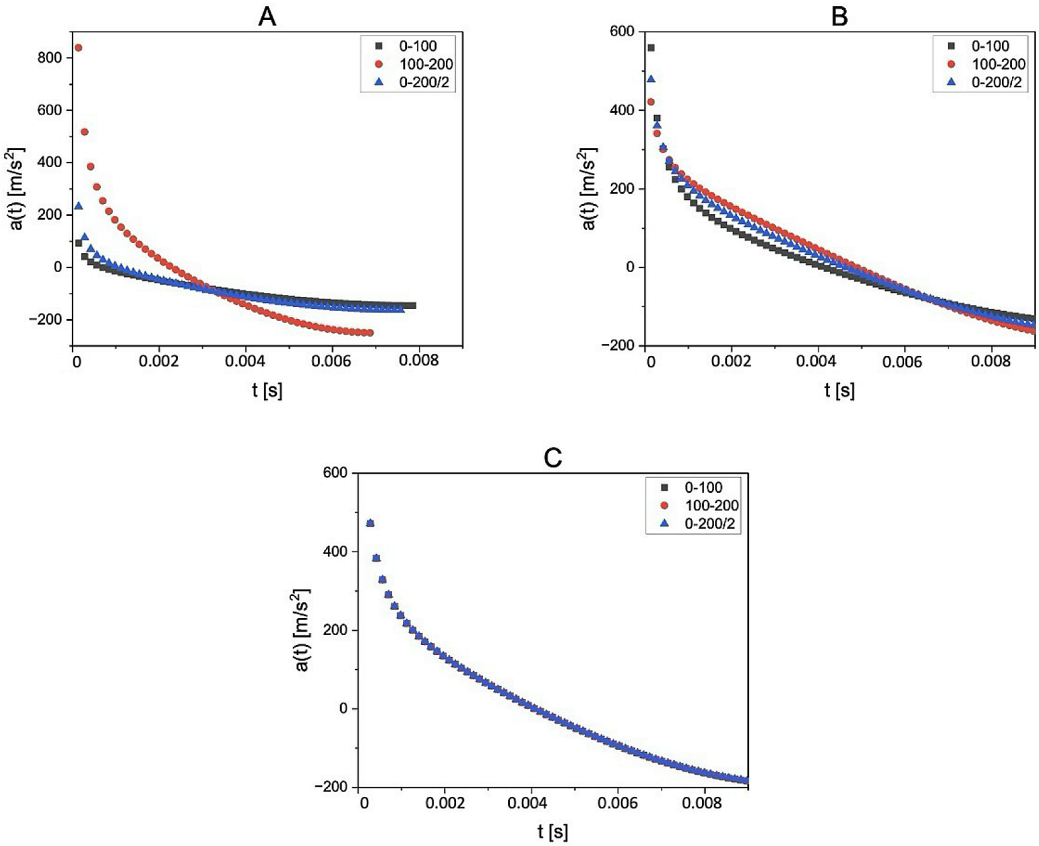

Figure 11. Acceleration of cut seat belt webbing under impact loading at drop heights: A – 1 m; B – 1.5 m; C – 2 m

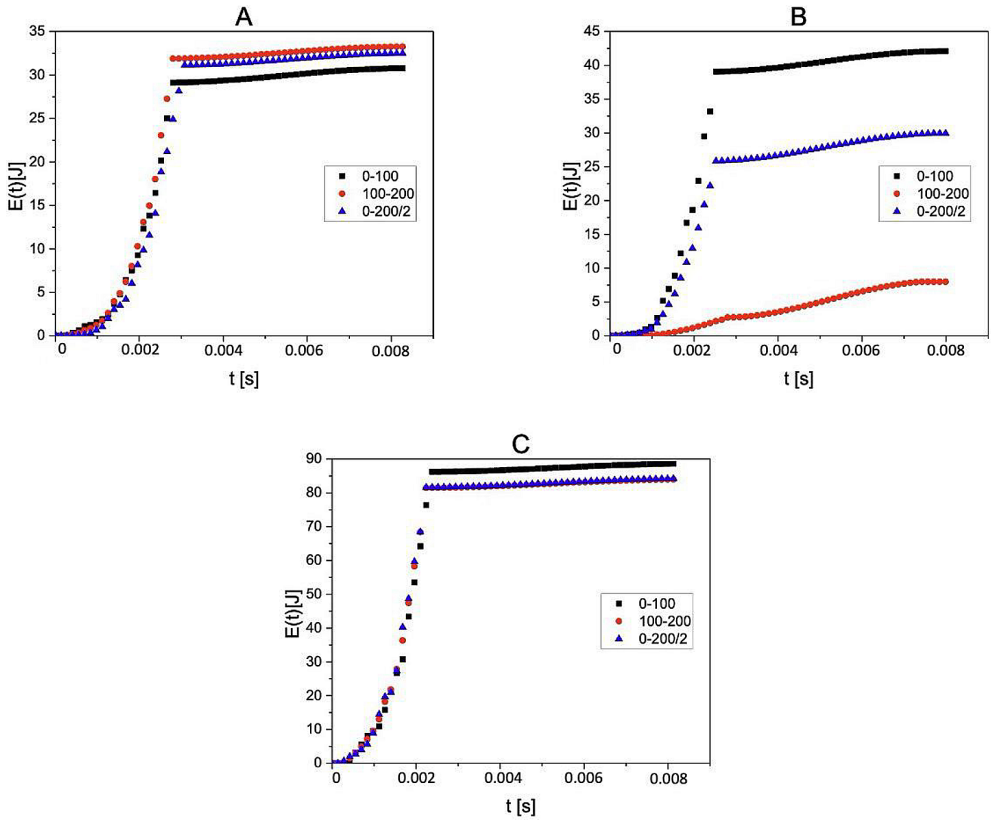

Figure 12. Elastic energy of new seat belt webbing under impact loading at drop heights: A – 1 m; B – 1.5 m; C – 2 m

average absorbed energy exceeded that of the other sections, suggesting non-uniform energy dissipation across the specimen, influenced by the instantaneous strain rate of the belt.

The corresponding results for the heated belt are shown in Figure 13. At a drop height of 1 m (Figure 13A), the absorbed energy (~33 J) was comparable to that of the new belt, though differences among the three measured sections (0–100 mm, 100–200 mm, 0–200/2 mm) were less pronounced. This may indicate localized changes in the mechanical properties of the material induced by heating, such as fibber weakening or increased thermal sensitivity of polyester yarns. At 1.5 m (Figure 13B), the absorbed energy increased most noticeably in the 0–100 mm section, i.e., the region closest to the clamping point. However, at 2 m (Figure 13C), a sharp reduction in absorbed energy was observed in all sections, with total values not exceeding 8 J. This unambiguously suggests structural degradation of the webbing and a significant loss of its ability to absorb impact energy, confirming that thermal conditioning adversely affects the protective capacity of the belt. For the cut belt, a significant deterioration in its ability to accumulate impact energy was observed, particularly at lower impact energy levels (Figure 14). At a drop height of 1 m (Figure 14A), all measured regions of the specimen reached a maximum energy of approximately 40 J. At 1.5 m (Figure 14B), a similar trend was noted, with the maximum energy increasing to around 64 J. However, at the highest drop height of 2 m (Figure 14C), substantial discrepancies between the measured sections became apparent. These differences indicate progressive belt degradation and suggest that the load-bearing capacity of the belt became non-uniform. Such irregular energy dissipation strongly undermines the reliability of the belt during real accident scenarios, representing a potentially severe risk to occupant protection.

Based on the analysis of the absorbed (dissipated) energy curves for the three belt conditions—new, thermally conditioned, and cut—it can be concluded that both mechanical damage and thermal exposure significantly affect the belt's ability to accumulate and dissipate energy. The new belt exhibited the most stable mechanical characteristics, although it still demonstrated sensitivity to strain rate. The heated belt revealed a clear reduction in stiffness and energy absorption capacity at higher load levels, with its response

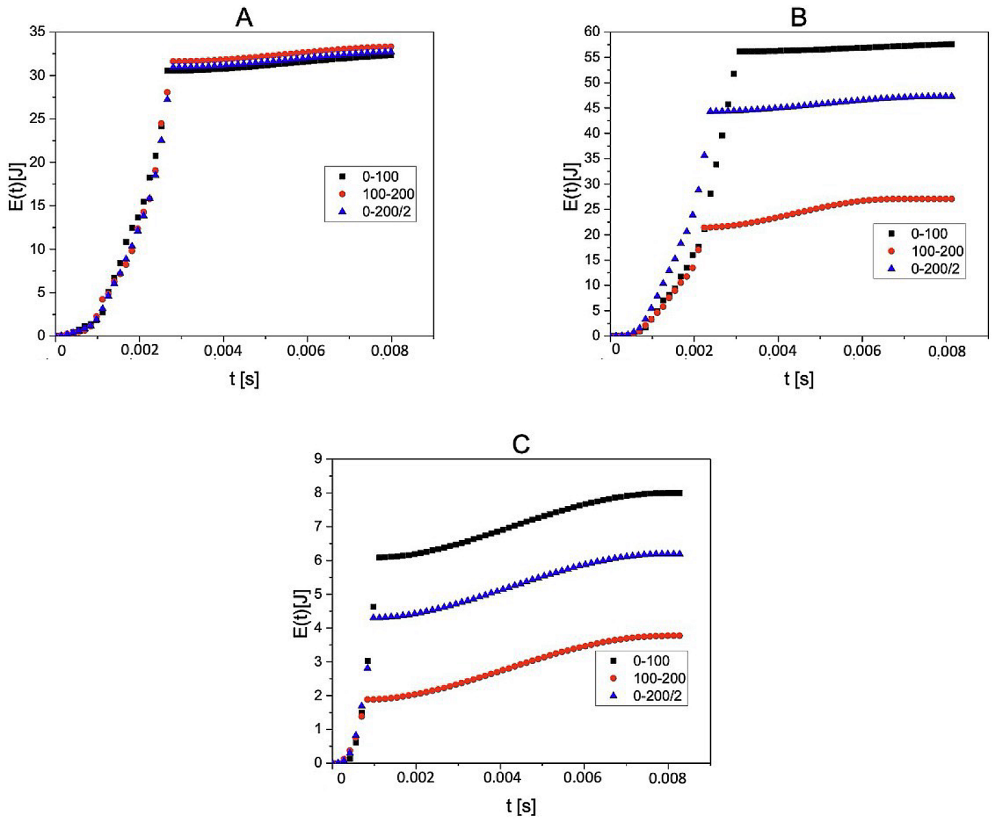

Figure 13. Elastic energy of heated seat belt webbing under impact loading at drop heights: A – 1 m; B – 1.5 m; C – 2 m

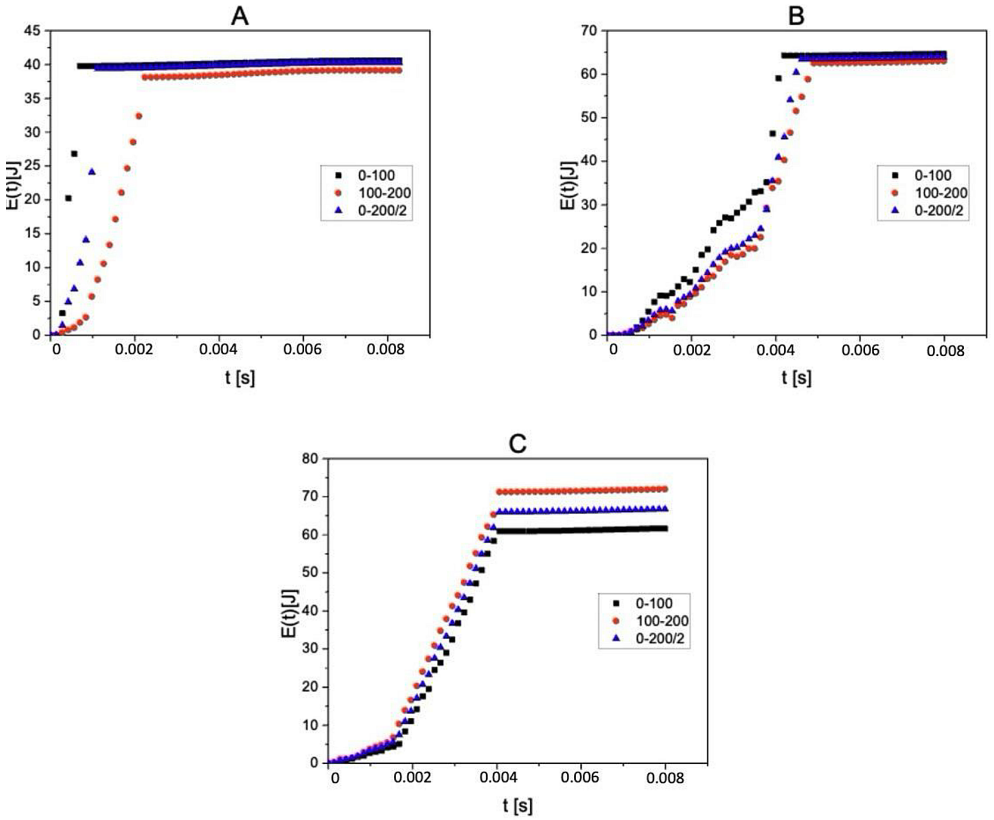

Figure 14. Elastic energy of cut seat belt webbing under impact loading at drop heights: A – 1 m; B – 1.5 m; C – 2 m

becoming increasingly unstable. The cut belt showed the most pronounced degradation, with localized defects leading to irregular and non-uniform energy dissipation. These results clearly demonstrate that both thermal degradation and mechanical damage can drastically reduce the effectiveness of seat belts in real-world crash scenarios, undermining their protective function.

For the new seat belt webbing, the results demonstrated relatively stable mechanical characteristics across all tested drop heights. The belt was capable of effectively accumulating and dissipating impact energy, although some sensitivity to strain rate was observed. At the highest impact level (2 m), the webbing absorbed up to ~90 J, with clear variation across measurement zones, suggesting a non-uniform distribution of strain energy. This finding is consistent with earlier reports indicating that the dynamic stiffness of polymer-based webbings depends strongly on deformation velocity. Nonetheless, the overall behaviour of the new webbing confirmed its ability to provide consistent protection under dynamic loading, validating its role as the primary energy-dissipating element in the restraint system.

In contrast, the thermally degraded seat belt webbing exhibited markedly reduced energy absorption capacity, particularly at higher impact levels. While the response at 1 m drop height was comparable to that of the new belt (~33 J), energy absorption drastically decreased to less than 8 J for the 2 m drop. This result clearly indicates a loss of structural integrity and a diminished ability to dissipate impact forces, most likely due to heat-induced weakening of polyester fibers. Local changes in material microstructure, such as fibber embrittlement or reduced inter-fibber cohesion, could explain the irregularities observed in the energy distribution across different belt zones. These findings strongly suggest that exposure of seat belt webbings to elevated temperatures, whether from environmental conditions or vehicle fires, may compromise their safety performance even before visible signs of damage appear.

The notched seat belt webbing presented yet another failure mode. At lower impact energies (1 m), the belt retained a moderate energy absorption capacity (~40 J), but increasing the impact severity led to both higher variability and indications of uneven energy distribution. At 2 m, the notched belt reached ~70 J in certain regions, but the irregular pattern of energy accumulation suggests local stress concentrations and premature fibber rupture. This non-uniform behaviour is particularly concerning, as it indicates that mechanical damage such as cuts or abrasions may cause unpredictable and localized failures, which could severely compromise the reliability of restraint systems during real-world crashes.

From a practical standpoint, these findings emphasize that both thermal degradation and mechanical damage can significantly reduce the protective efficiency of seat belts. While a new belt can reliably dissipate impact energy, belts subjected to high temperatures or cuts exhibit severe performance deterioration, in some cases losing their energy-absorbing capacity almost entirely. This raises important concerns regarding the long-term durability of seat belts in vehicles exposed to harsh conditions and highlights the need for routine inspection and timely replacement of damaged webbings.

The study also has broader implications for automotive safety standards. Current regulatory frameworks focus primarily on new components, but do not sufficiently account for in-service degradation mechanisms. The results of this work suggest that incorporating degradation-related testing (e.g., after thermal exposure or controlled notching) could provide a more realistic assessment of seat belt reliability.

Finally, it is important to note some limitations of this study. The experiments were conducted on simplified specimens with a limited gauge length and using a drop tower system, which does not fully replicate the complex boundary conditions of seat belts in real vehicles. Furthermore, only a single type of thermal treatment and notch geometry were considered. Future work should therefore expand to include other environmental factors (UV exposure, humidity), varied damage types, and full-scale seat belt assemblies. Advanced numerical simulations may also help in understanding the localized stress distributions and predicting failure modes under realistic crash conditions.

The results demonstrate that seat belt webbings are highly sensitive to both mechanical and thermal degradation. While new belts show stable and efficient energy dissipation, degraded belts may lose their protective capacity, leading to a significant increase in occupant injury risk. These findings underline the critical importance of monitoring the condition of seat belts throughout their service life and incorporating degradation effects into both design practices and safety regulations.

CONCLUSIONS

This study investigated the dynamic behaviour of seat belt webbing in three conditions: new, thermally degraded, and mechanically notched. The main findings can be summarized as follows:

1. New webbing exhibited stable mechanical response and the highest capacity for energy absorption and dissipation, confirming its effectiveness as a protective element of restraint systems.
2. Thermally degraded webbing showed a drastic reduction in stiffness and energy dissipation capacity at higher impact energies, indicating that elevated temperature exposure significantly compromises belt performance.
3. Mechanically notched webbing demonstrated localized and irregular deformation, with energy absorption distributed unevenly across the specimen. This suggests that even small cuts can critically reduce reliability during crash events.
4. Both types of degradation – thermal and mechanical – may severely reduce the safety margin of seat belt systems, increasing the risk of failure under real accident conditions.
5. Overall, the results highlight the importance of monitoring seat belt condition throughout service life. The findings support the need to include degradation-related scenarios in future testing protocols and regulatory standards. Future research should address additional degradation factors, such as UV exposure and aging, and extend to full-scale belt assemblies and numerical modeling for predictive assessment of crash performance.

REFERENCES

1. Alexa V. Testing of automotive industry products using mechatronic systems. Acta Tech Corviniensis-Bull Eng. 2019;12(3):73–5.
2. Łabęcka, M, Żaba, C, Lorkiewicz-Muszyńska, D, Świderski, P, Mularski, A, Kołowski, J. Obrażenia śmiertelne narządów szyi spowodowane zapiętymi pasami bezpieczeństwa (in Polish). Arch. Med. Sąd. Kryminol, 2011; 170–175.
3. Ungureanu S, Muresan CO, Enache A, Ciocan V, Stan E, Dumache R, et al. Medico-legal considerations of seat belt syndrome with severe abdominal trauma: A case report and literature review. Cureus, 2025, Aug 24. https://doi.org/10.7759/cureus.90902
4. Krawiec P, Warguła Ł, Małozięć D, Kaczmarzyk P, Dziechciarz A, Czarnecka-Komorowska D. The toxicological testing and thermal decomposition of drive and transport belts made of thermoplastic multilayer polymer materials. Polymers, 2020; 12(10):2232. https://doi.org/10.3390/polym12102232
5. https://www.ecfr.gov/current/title-49/part-571/section-571.302).
6. Li D (Xuedong). Fundamental of fibers. In: Cut Protective Textiles. Elsevier; 2020, p. 59–110 [cited 2025 Aug 31]. Available from: https://linkinghub.elsevier.com/retrieve/pii/B9780128200391000031 doi:10.1016/B978-0-12-820039-1.00003-1
7. Gong X, Chen X, Zhou Y. Advanced weaving technologies for high-performance fabrics. In: High-Performance Apparel. Elsevier; 2018, p. 75–112 [cited 2025 Aug 31]. Available from: https://linkinghub.elsevier.com/retrieve/pii/B9780081009048000043 https://doi.org/10.1016/B978-0-08-100904-8.00004-3
8. Hari PK. Types and properties of fibres and yarns used in weaving. In: Woven Textiles. Elsevier; 2012, p. 3–34 [cited 2025 Aug 31]. Available from: https://linkinghub.elsevier.com/retrieve/pii/B9781845699307500013 doi:10.1533/9780857095589.1.3
9. Sobolewski T, Trzaska P. Bezpieczeństwo pasażerów autobusów w kontekście obowiązujących przepisów homologacyjnych foteli autobusowych (in Polish). Logistyka. 2012; (3, CD 1): 2061–2069.
10. Steptoe A, Wardle J, Fuller R, Davidsdottir S, Davou B, Justo J. Seatbelt use, attitudes, and changes in legislation. Am J Prev Med. 2002; 23(4):254–9. https://doi.org/10.1016/S0749-3797(02)00513-5
11. Høye A. How would increasing seat belt use affect the number of killed or seriously injured light vehicle occupants? Accid Anal Prev. 2016; 88:175–86. doi:10.1016/j.aap.2015.12.022
12. Łabecka M, Zaba C, Lorkiewicz-Muszyńska D, Swiderski P, Mularski A, Kołowski J. Fatal injuries of organs situated in the neck caused by fastened seat belts. Arch Med Sadowej Kryminol. 2011; 61(2):170–5. PubMed PMID: 22390131.
13. Gierczycka D, Cronin DS. Occupant thorax response variations due to arm position and restraint systems in side impact crash scenarios. Accid Anal Prev. 2017; 106:173–80. https://doi.org/10.1016/j.aap.2017.05.017
14. Intas G, Stergiannis P. Seat belt syndrome: a global issue. Health Sci J. 2010; 4(4):202.
15. Masudi T, McMahon H, Scott J, Lockey A. Seat belt-related injuries: A surgical perspective. J Emerg Trauma Shock. 2017; 10(2):70. https://doi.org/10.4103/0974-2700.201590
16. Al-Ozaibi L, Adnan J, Hassan B, Al-Mazroui A, Al-Badri F. Seat belt syndrome: Delayed or missed

intestinal injuries, a case report and review of literature. Int J Surg Case Rep. 2016; 20:74–6. https://doi.org/10.1016/j.ijscr.2016.01.015

17. Garrett JW, Braunstein PW. The seat belt syndrome. J Trauma Acute Care Surg. 1962; 2(3):220–38.
18. Wotherspoon S, Chu K, Brown AF. Abdominal injury and the seat-belt sign: Seat-belt sign. Emerg Med. 2001; 13(1):61–5. https://doi.org/10.1046/j.1442-2026.2001.00180.x
19. Stassen NA. Abdominal seat belt marks in the era of focused abdominal sonography for trauma. Arch Surg. 2002; 137(6):718. https://doi.org/10.1001/archsurg.137.6.718
20. Chandler CF, Lane JS, Waxman KS. Seatbelt sign following blunt trauma is associated with increased incidence of abdominal injury. Am Surg. 1997; 63(10):885–8. PubMed PMID: 9322665.
21. Duma SM, Kemper AR, Stitzel JD, Mcnally C, Kennedy EA, Matsuoka F. Rib fracture timing in dynamic belt tests with human cadavers. Clin Anat. 2011; 24(3):327–38. https://doi.org/10.1002/ca.21130
22. Alexandru GI, Marius CG, Daniel TF, Dragos TD. Dynamics of frontal crash in/without the presence of passive safety systems. In: IOP Conf. Ser.: Mater. Sci. Eng. 2022; 1220:012044. https://doi.org/10.1088/1757-899X/1220/1/012044.
23. Jackowski J, Wieczorek M, Żmuda M. Badania obciążeń dynamicznych kierowcy pojazdu podczas zderzenia czołowego (in Polish). TTS Tech Transp Szyn. 2013; 20.
24. Maćkowiak P, Kotyk M, Boroński D. Construction of a test stand and a method for the assessment of safety belts' mounting points in terms of valid rules. Problemy Eksploatacji, 2016, 3, 35-42.
25. Itu C, Toderita A, Melnic LV, Vlase S. Effects of seat belts and shock absorbers on the safety of racing car drivers. Mathematics, 2022; 10(19):3593. https://doi.org/10.3390/math10193593
26. Dunn RF, McSwain RH, Mills T, Malone B. Failure of plastic press release buttons in automobile seat belts. Eng Fail Anal. 2005; 12(1):81–98. https://doi.org/10.1016/j.engfailanal.2004.05.003
27. Żuchowski A, Prochowski L, Zielonka K. Analiza wpływu elastyczności taśmy pasa na bezpieczeństwo pasażerów autobusów (analiza przemieszczeń pasażerów) (in Polish). Logistyka. 2015; (4, CD 2):7106–15.
28. Muszyński A, Trzaska P, Wicher J, Mazurkiewicz Ł. Analiza sił działających w taśmach pasów podtrzymujących dziecko w foteliku bezpieczeństwa (in Polish). Arch Motoryz. 2015; 67(1):239–52.
29. Sybilski K, Fernandes FAO, Ptak M, Alves de Sousa RJ. Injury biomechanics evaluation of a driver with disabilities during a road accident—A numerical approach. Materials, 2022; 15:7956. https://doi.org/10.3390/ma15227956